
Proton Affinity of Uracil. A Computational Study of Protonation Sites

Jill K. Wolken and František Tureček*

Department of Chemistry, University of Washington, Seattle Washington, USA

Relative stabilities of uracil tautomers and cations formed by gas-phase protonation were studied computationally with the B3LYP, MP2, QCISD, and QCISD(T) methods and with basis sets expanding from 6-31G(*d,p*) to 6-311+G(3*df*,2*p*). In accordance with a previous density functional theory study, the dioxo tautomer **1a** was the most stable uracil isomer in the gas phase. Gibbs free energy calculations using effective QCISD(T)/6-311+G(3*df*,2*p*) energies suggested >99.9% of **1a** at equilibrium at 523 K. The most stable ion isomer corresponded to *N*-1 protonated 2,4-dihydropyrimidine, which however is not formed by direct protonation of **1a**. The topical proton affinities in **1a** followed the order O-8 > O-7 > C-5 > N-3 > N-1. The thermodynamic proton affinity of **1a** was calculated as 858 kJ mol⁻¹ at 298 K. A revision is suggested for the current estimate included in the ion thermochemistry database. (J Am Soc Mass Spectrom 2000, 11, 1065–1071) © 2000 American Society for Mass Spectrometry

The thermochemistry of gas-phase ions derived from biologically important molecules has been studied extensively, in particular following the advent of soft ionization methods such as electrospray [1] and matrix-assisted laser desorption [2] that allow for facile formation of large ions in the gas phase. With ions formed by protonation, the gas-phase basicity and proton affinity are the two most important energy values that link the ion thermochemistry to that of neutral molecules. Unfortunately, proton affinities of polar multifunctional molecules, an attribute common to most biologically interesting molecules such as amino acids, peptides, nucleobases, nucleosides, etc., are difficult to measure by reliable experimental methods that are based on low pressure equilibria in ion-cyclotron resonance mass spectrometers [3], or high-pressure equilibria in pulse ionization methods [4, 5]. Most experimental data produced so far originated from competitive dissociations of proton-bound dimers (the kinetic method) [6]. In addition, experimental methods based on either equilibrium or kinetic measurements probe the most stable ion structures corresponding to protonation at the most basic sites in the molecule. Hence, topical proton affinities of less basic sites in multifunctional molecules are difficult to obtain by experimental methods.

Our interest in topical proton affinities is motivated by the use of ion–molecule reactions to generate well defined ion structures that can be used as precursors for the generation of transient radicals by fast electron

transfer [7]. In this context, ab initio and density functional theory have been used previously to obtain topical proton affinities for several systems [8–11]. In the present work we report calculations investigating the gas-phase protonation of the RNA nucleobase uracil (**1**). Uracil is an interesting model in that it can exist in several tautomers each providing several potential protonation sites leading to a multitude of ion isomers. The goal of this work was to determine the structures and energetics of protonated uracil isomers and draw conclusions on the formation of gas-phase ions by protonation of uracil. Topical proton affinities in the most stable uracil tautomer have been addressed previously at various levels of theory [12–14]. The present work provides a comprehensive view of protonated uracil isomers. It is the first study to address the stabilities of both neutral and cation tautomers at a high level of theory. Very recent MP4(SDTQ)/6-31+G(*d,p*) calculations reported the proton affinity of uracil as 857 kJ mol⁻¹ in agreement with our results [15].

Calculations

Standard calculations were performed using the Gaussian 94 [16] and Gaussian 98 [17] suites of programs. Geometries were optimized with HF/6-31G(*d,p*) to obtain local energy minima that were characterized by harmonic frequency analyses (all frequencies real). HF frequencies were scaled by 0.893 [18] and used to calculate zero-point energy and 298 K enthalpy corrections. Selected structures were also optimized with density functional theory [19, 20] calculations using Becke's hybrid functional (B3LYP) [21, 22] and the 6-31+G(*d,p*) basis set including vibrational analysis.

Address reprint requests to Professor František Tureček, Department of Chemistry, Bagley Hall, Box 351700, University of Washington, Seattle, WA 98195-1700

The B3LYP harmonic frequencies were scaled by 0.963 [23]. Vibrational enthalpies were treated within the rigid-rotor-harmonic oscillator approximation. Spin restricted calculations were used for all closed-shell systems. Improved energies were obtained from single-point calculations at several levels of theory. Moller–Plesset perturbational theory [24] truncated at second order, MP2(frozen core), was used with the 6-311G(2*d,p*), 6-311+G(2*d,p*), 6-311+G(2*df,p*), and 6-311+G(3*df,2p*) basis sets to account for correlation energy effects. In addition, two composite procedures were adopted that consisted of quadratic configuration interaction calculations [25], QCISD/6-31G(*d,p*) and QCISD(T)/6-31G(*d,p*), and basis set expansions through MP2 calculations to an effective QCISD/6-311+G(2*d,p*), QCISD(T)/6-311+G(2*df,p*), and QCISD(T)/6-311+G(3*df,2p*) levels of theory according to

$$\begin{aligned} \text{QCISD}/6\text{-}311+\text{G}(2d,p) &\approx \text{QCISD}/6\text{-}31\text{G}(d,p) \\ &+ \text{MP2}/6\text{-}311+\text{G}(2d,p) \\ &- \text{MP2}/6\text{-}31\text{G}(d,p) \end{aligned} \quad (1)$$

$$\begin{aligned} \text{QCISD(T)}/6\text{-}311+\text{G}(2df,p) &\approx \text{QCISD(T)}/6\text{-}31\text{G}(d,p) \\ &+ \text{MP2}/6\text{-}311+\text{G}(2df,p) \\ &- \text{MP2}/6\text{-}31\text{G}(d,p) \end{aligned} \quad (2)$$

$$\begin{aligned} \text{QCISD(T)}/6\text{-}311+\text{G}(3df,2p) &\approx \text{QCISD(T)}/6\text{-}31\text{G}(d,p) \\ &+ \text{MP2}/6\text{-}311+\text{G}(3df,2p) \\ &- \text{MP2}/6\text{-}31\text{G}(d,p) \end{aligned} \quad (3)$$

Similar effective levels of theory, that are analogous to the Gaussian 2(MP2) [26] and (MP2,SVP) [27] schemes, were used previously for treating the energetics of several heterocyclic molecules, ions, and radicals [7, 28–32]. Density functional theory calculations were also performed using Becke's hybrid functional (B3LYP) and the 6-311G(2*d,p*), 6-311+G(2*d,p*), and 6-311+G(2*df,p*) basis sets. We showed previously that simple averaging of MP2 and B3LYP relative energies provided an improved fit to experimental data for several radical and cationic systems [11, 28–32] and the method (denoted B3-MP2) has recently been used successfully to calculate gas-phase acidities and anion relative energies [33].

Results and Discussion

The two carbonyl groups in uracil allow the existence of several tautomers that have been studied previously by theory, as summarized recently [34]. The HF/6-31G(*d,p*) optimized structures of the six lowest-energy tautomers **1a–1f** were unexceptional and showed standard bond lengths and angles in line with previous calculations. A similar conclusion followed from the

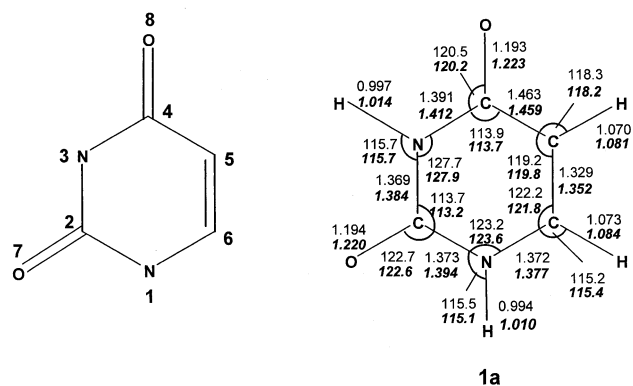


Figure 1. Optimized geometry of **1a**. Bond lengths in angstroms, bond and dihedral angles in degrees. Roman numerals: HF/6-31G(*d,p*) parameters. Bold italics: B3LYP/6-31+G(*d,p*) parameters.

comparison of the HF and B3LYP-optimized structures for **1a** that showed only minor differences (Figure 1). Previous calculations and experimental studies [35–48] agreed on structure **1a** as the most stable uracil tautomer. The present calculations identified **1a** (Figure 1) and the next five most stable uracil tautomers as shown in Figure 2. The dioxo tautomer **1a** was the most stable structure at all present levels of theory. The energy differences discussed in the text refer to 298 K relative enthalpies from effective QCISD/6-311+G(2*d,p*) calculations. The relative enthalpies from the other calculations are summarized in Table 1. Enolization of the N-1–C-2–O-7 system led to the second most stable tautomer **1b**, which was 46 kJ mol^{−1} less stable than **1a**. Interestingly, enolization of the N-3–C-4–O-8 system was more destabilizing compared with that of the N-1–C-2–O-7 system and resulted in tautomer **1c**, which was 50 kJ mol^{−1} less stable than **1a**. Double enolization had a weak additional destabilizing effect, as shown by the 2,4-dihydropyrimidine structure **1d** which was 52 kJ mol^{−1} less stable than **1a**. The two least stable structures corresponded to the enaminoimide structure **1e** formed by enolization of the O-7–C-2–N-3 system, and the iminodienol structure **1f** formed by homoenolization of the O-8–C-4–C-5–C-6–N-1 system, which, respectively, were 77 and 103 kJ mol^{−1} less stable than **1a**.

The present results are in a qualitative agreement with a recent density functional study [33] that reported the same ordering of tautomer relative energies. However, the present calculations that were performed with larger basis sets and at higher levels of correlation energy treatment yielded somewhat different relative energies for the tautomers. In particular, the dihydropyrimidine structure **1d** was calculated to be less destabilized against **1a** than was reported by previous calculations and was thus closer in energy to **1c** and **1b** (Table 1). The calculated relative energies showed that including diffuse functions in the basis set had a small effect on the tautomer relative energies. The MP2,

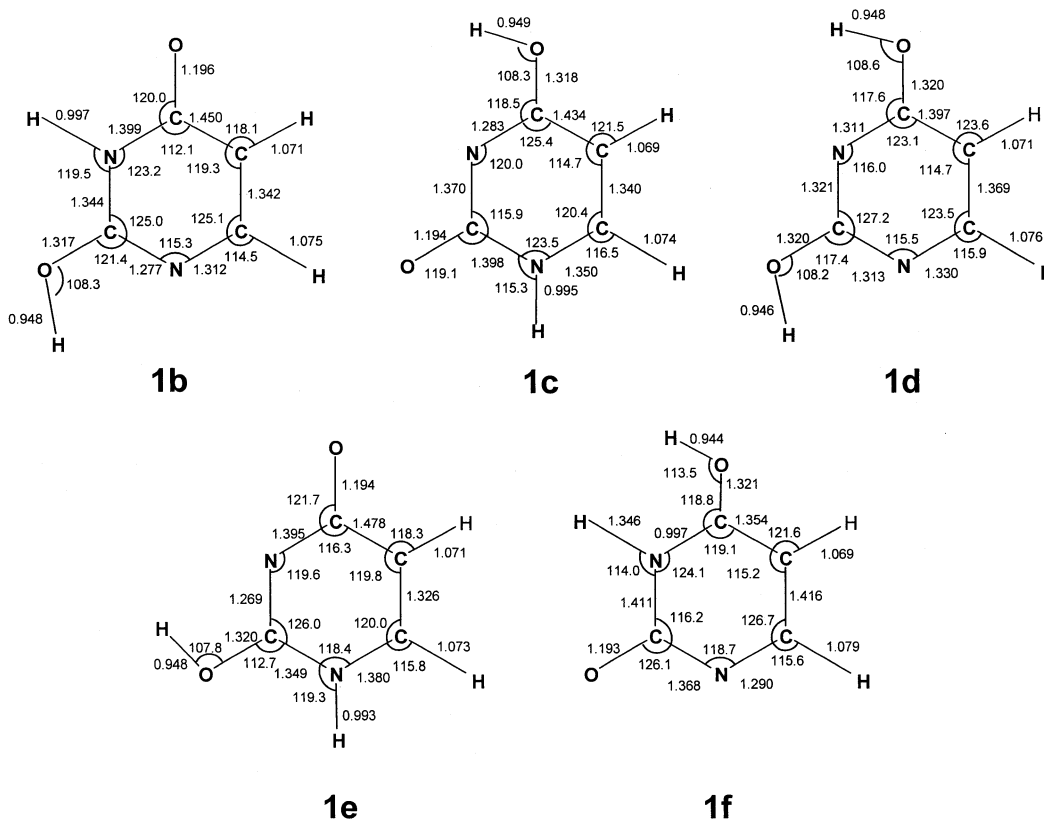


Figure 2. HF/6-31G(*d,p*) optimized geometries of **1b–1f**. Bond lengths in angstroms, bond and dihedral angles in degrees.

B3LYP, and QCISD relative energies were very similar, e.g., within 9 kJ mol⁻¹ absolute deviations and 4.9 and 2.6 kJ mol⁻¹ root-mean-square deviations for comparing the MP2 and B3LYP data, respectively, with those from the presumably “best” effective QCISD calculations. Considering that the above procedures use very different formalisms to account for electron correlation, the close consistency of the relative energies lends credit to the results.

The relative enthalpies together with the calculated entropies (S_T) were used to calculate the relative free energies and hence the equilibrium composition of the tautomer mixture in the gas phase. This was calculated for the typical temperature of a chemical ionization ion source used for uracil protonation (~523 K). Because

the S_{523} values were very similar for **1a–1f** (404–411 J mol⁻¹ K⁻¹), the equilibria were largely determined by the differences in the tautomer energies. For example, the free energy difference $\Delta G_{523}(\mathbf{1a} \rightarrow \mathbf{1b}) = 47.3$ kJ mol⁻¹ indicates that there should be 99.99% of the more stable tautomer **1a** at gas phase equilibrium at 523 K. Hence, gas-phase protonation of uracil is predicted to occur exclusively in the most stable tautomer **1a**.

Uracil Cations

Protonation of uracil tautomers can, in principle, take place at any C, N, or O atom to form tautomeric ions. The 18 most stable cation tautomers are shown in Figure 3. In addition, some ions existed as *syn* and *anti* rotamers differing in the dihedral angles of the O–H bonds. Only the more stable rotamers are listed here. The ion tautomers are marked according to the proton attachment sites, e.g., **178⁺** for the N-1 protonated dihydroxypyrimidine that was the most stable ion (Table 2). Note that ion **178⁺** can be formed convergently by protonating the N-1 position in **1d**, the O-7 position in **1c**, and the O-8 position in **1e**, but not by protonation of the two most stable uracil tautomers **1a** and **1b**. The protonation exothermicities are expressed as the topical proton affinities of the uracil tautomers and summarized in Table 3. The second most stable ion,

Table 1. Relative energies of uracil tautomers **1a–1f**

Method	Relative energy ^a					
	1a	1b	1c	1d	1e	1f
MP2/6-311G(<i>d,p</i>)	0	43	47	43	78	100
MP2/6-311+G(2 <i>d,p</i>)	0	43	47	43	75	99
B3LYP/6-311G(<i>d,p</i>)	0	47	49	52	82	99
B3LYP/6-311+G(2 <i>d,p</i>)	0	46	49	52	80	98
QCISD/6-31G(<i>d,p</i>)	0	48	55	48	83	108
QCISD/6-311+G(2 <i>d,p</i>)	0	46	50	52	77	103

^aIn units of kJ mol⁻¹ at 298 K.

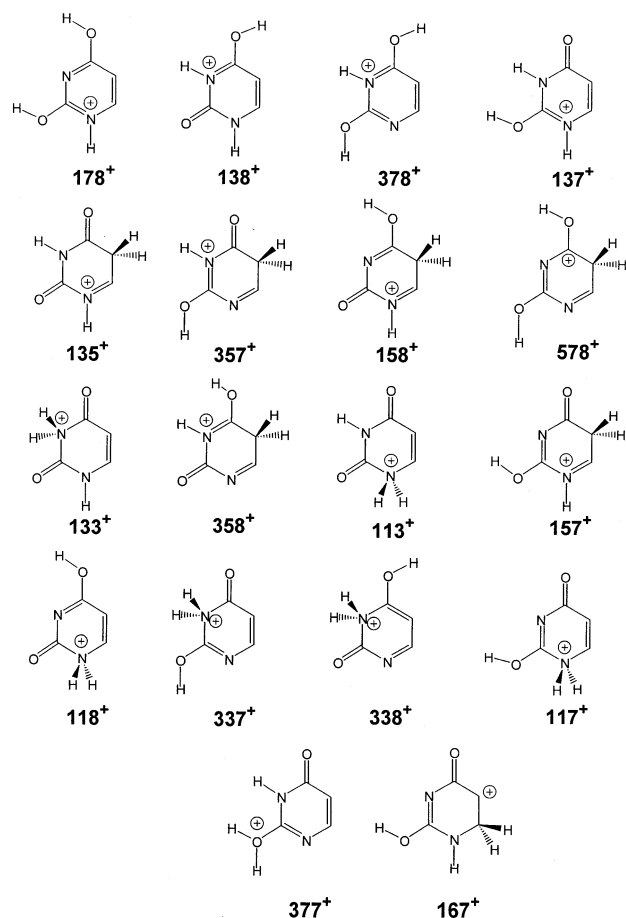


Figure 3. Structures of uracil cations.

Table 2. Relative energies of uracil cations

Cation	Relative energy ^{a,b}								
	B3LYP/ 6-311G(2d,p)	MP2/ 6-311G(2d,p)	B3LYP ^c 6-311+G(2df,p)	MP2 ^c 6-311+G(2df,p)	QCISD ^b 6-311+G(2d,p)	QCISD(T) ^c 6-311+G(2df,p)	QCISD(T) ^c 6-311+G(3df,2p)		
178 ⁺	0	0 ^d	0	0 ^d	0	0	0		
138 ⁺	5 (5) ^e	7	9 (9) ^e	4	7	10 (9) ^f	7	10	9
378 ⁺	31 (30) ^e	32	32 (32) ^e	31	32	32 (32) ^f	33	32	32
137 ⁺	45 (45) ^e	44	44 (44) ^e	43	43	44 (42) ^f	38	42	40
135 ⁺	86 (86) ^e	84	83 (83) ^e	87	87	88 (87) ^f	72	83	82
357 ⁺	100	101	102						
158 ⁺	120	119	118						
578 ⁺	122	126	130						
133 ⁺	130 (131)	128	125 (125)				124		
358 ⁺	142	140	139						
113 ⁺	150 (149)	144	139 (144)				132		
157 ⁺	168	168	168						
118 ⁺	172	170	168						
337 ⁺	199	196	194						
338 ⁺	221	221	221						
117 ⁺	236	231	226						
377 ⁺	340	337	335						
167 ⁺	334	352	369						

^aIn units of kJ mol⁻¹ at 298 K.

^bFrom single-point calculations on HF/6-31G(*d,p*) optimized structures and using HF/6-31G(*d,p*) zero-point energies and 298 K enthalpies.

^cFrom single-point calculations on B3LYP/6-31+G(*d,p*) optimized structures and using B3LYP/6-31+G(*d,p*) zero-point energies and 298 K enthalpies.

^dAveraged B3-MP2 relative energies.

^eCalculated with the 6-311+G(2*d,p*) basis set.

^fCalculated with the 6-311+G(3*df*,2*p*) basis set.

138⁺, was only 5–10 kJ mol⁻¹ less stable than isomer 178⁺ at several levels of theory (Table 2). Ion 138⁺ can also be formed by protonation of O-8 in 1a, N-3 in 1c, or N-1 in 1f. Protonation at O-7 in 1a was 30–35 kJ mol⁻¹ less exothermic than at O-8 so that ion 137⁺ was the fourth most stable isomer. Note that ion 137⁺ can also be formed by protonation at N-1 in 1b. Protonation at C-5 in 1a–1d was generally less favorable than at the heteroatoms. For example, isomer 135⁺ formed by protonation of 1a at C-5 was 72 kJ mol⁻¹ less stable than the most stable isomer 178⁺.

Protonation at C-5 can be accommodated by the electronic system of the pertinent uracil tautomer to form ions that can be expressed by conjugated canonical structures, e.g., 135⁺, 357⁺, 158⁺, 578⁺, 358⁺, and 157⁺ that all represent stable ion structures. By contrast, protonation at C-6 forms an α -carbonyl carbocation moiety at C-5 that is known to be strongly destabilizing in aliphatic [49] and heterocyclic cations [29]. Consequently, starting structures in which a proton was attached to C-6 often underwent spontaneous isomerization by proton migration to C-5 or N-1. The only stable C-6- protonated ion structure found by the present study was that for ion 167⁺, which was a high-energy isomer destabilized against 178⁺ by >350 kJ mol⁻¹ (Table 2) and thus of little practical importance.

Protonation at the hydroxyl groups and amide nitrogen atoms was also less favorable. The O-7-H group in 1b was the most basic one of those studied, and its protonation formed the high-energy ion 377⁺. The N-3

Table 3. Topical proton affinities in **1a–1f**^a

Tautomer	Method	Position				
		N-1	N-3	C-5	O-7	O-8
1a	MP2/6-311G(2 <i>d,p</i>)	735	750	792	831	865
	B3LYP/6-311G(2 <i>d,p</i>)	734	753	797	838	878
	MP2/6-311+G(2 <i>d,p</i>)	718	732	775	813	848
	B3LYP/6-311+G(2 <i>d,p</i>)	718	737	782	822	863
	MP2/6-311+G(2 <i>df,p</i>)			767	812	845
	MP2/6-311+G(3 <i>df,2p</i>)			769	815	848
	B3LYP/6-311+G(2 <i>df,p</i>)			780	824	863
	B3-MP2/6-311+G(2 <i>df,p</i>)			773	818	854
	QCISD/6-311+G(2 <i>d,p</i>)	731	738	792	825	857
	QCISD(T)/6-311+G(2 <i>df,p</i>)			782	824	855
QCISD(T)/6-311+G(3 <i>df,2p</i>)			784	826	858	
1b	MP2/6-311G(2 <i>d,p</i>)	917	886	787		
	B3LYP/6-311G(2 <i>d,p</i>)	935	899	813		
	MP2/6-311+G(2 <i>d,p</i>)	901	869			
	B3LYP/6-311+G(2 <i>d,p</i>)	920	890			
	QCISD/6-311+G(2 <i>d,p</i>)	916	883			
1c	MP2/6-311G(2 <i>d,p</i>)	754	854	804	917	
	B3LYP/6-311G(2 <i>d,p</i>)	760	867	812	935	
	MP2/6-311+G(2 <i>d,p</i>)		836		901	
	B3LYP/6-311+G(2 <i>d,p</i>)		851		920	
	QCISD/6-311+G(2 <i>d,p</i>)		897		916	
1d	MP2/6-311G(2 <i>d,p</i>)	917	886	788		
	B3LYP/6-311G(2 <i>d,p</i>)	935	899	813		
	MP2/6-311+G(2 <i>d,p</i>)	901	869			
	B3LYP/6-311+G(2 <i>d,p</i>)	920	890			
	QCISD/6-311+G(2 <i>d,p</i>)	916	884			
1e	MP2/6-311G(2 <i>d,p</i>)	726	874	784	583	952
	B3LYP/6-311G(2 <i>d,p</i>)	729	884	797	631	965
	MP2/6-311+G(2 <i>d,p</i>)		889			933
	B3LYP/6-311+G(2 <i>d,p</i>)		902			947
	QCISD/6-311+G(2 <i>d,p</i>)		902			941
1f	MP2/6-311G(2 <i>d,p</i>)	953	754	835	925	904
	B3LYP/6-311G(2 <i>d,p</i>)	965	761	839	934	914
	MP2/6-311+G(2 <i>d,p</i>)	935			907	
	B3LYP/6-311+G(2 <i>d,p</i>)	949			917	
	QCISD/6-311+G(2 <i>d,p</i>)	948			917	

^aIn units of kJ mol⁻¹ at 298 K.

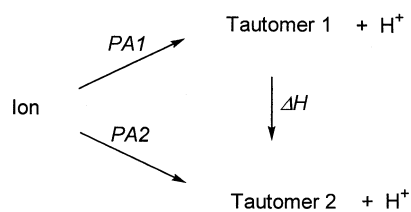
site in **1a** was the most basic amide nitrogen that upon protonation formed stable ion **133**⁺.

The effects of basis set expansion and improved levels of correlation energy treatment were investigated for the five most stable ion isomers **178**⁺, **138**⁺, **378**⁺, **137**⁺, and **135**⁺ (Table 2). In general, the MP2 and B3LYP relative energies calculated with the 6-311G(2*d,p*) and 6-311+G(2*d,p*) basis sets showed very good agreement, which was within 3 kJ mol⁻¹ absolute deviation. Averaging the relative energies by B3-MP2 therefore did not result in significant improvement. Further expansion of the basis set up to 6-311+G(3*df,2p*) had a negligible effect on the ion relative energies. Including quadratic configuration interaction also had a small effect on the ion relative energies. For example the B3-MP2 relative energies were within 3–4 kJ mol⁻¹ absolute of the extrapolated

QCISD(T)/6-311+G(3*df,2p*) values (Table 2). It appears that reliable B3-MP2 relative energies can be obtained for protonated uracil tautomers with the economical 6-311G(2*d,p*) basis set. This is promising for investigations of larger systems for which higher-level QCISD or QCISD(T) single-point calculations are still prohibitively expensive in terms of computational time and memory requirements.

Topical and Thermodynamic Proton Affinities

Combining the uracil tautomer relative enthalpies with those of the ions allows one to calculate the 298 K proton affinities and rank the neutral tautomers by their basicity in the gas phase (Table 3). Note that not all topical proton affinities are listed explicitly in Table 3. The PA values not listed can be obtained readily from



thermochemical cycles using the relative energies of uracil tautomers from Table 1 (Scheme 1). For example, the topical proton affinity of **1b** at O-8 is equal to the proton affinity of tautomer **1f** at O-7 plus the energy difference $\Delta H(\mathbf{1b}) - \Delta H(\mathbf{1f})$ (Table 1). Because only the most stable uracil tautomer **1a** exists in the gas-phase at thermal equilibrium, only the topical proton affinities in **1a** are of practical importance as far as direct uracil protonation is concerned, and therefore are discussed here. Table 3 shows the calculated proton affinities of the potential protonation sites in **1a**, which decrease in the order O-8 > O-7 > C-5 > N-3 > N-1. The proton affinity of the most basic site was studied at several levels of theory including basis set expansions for the B3LYP, MP2, and effective QCISD and QCISD(T) schemes. The energies calculated with the hybrid B3LYP method were insensitive to basis set expansion that added valence shells and polarization functions, e.g., from 6-31+G(*d,p*) to 6-311+G(2*df,p*). The energies calculated with the MP2(frozen core) showed a decrease upon adding valence shell, polarization, and diffuse functions [e.g., from 6-31G(*d,p*) to 6-311+G(2*df,p*)], followed by a small increase upon further basis set expansion. Treating **1a** and **138⁺** with QCISD(T) further stabilized the larger electronic system of the ion leading to an increased proton affinity. At the highest level of theory, which in this work was effective QCISD(T)/6-311+G(3*df,2p*), we obtain PA(uracil) = 858 kJ mol⁻¹ (Table 3). This value is very well reproduced by the B3-MP2 datum (854 kJ mol⁻¹) and the B3LYP values (861–863 kJ mol⁻¹). Previous calculations using B3LYP and Moller–Plesset theory with relatively small basis sets of split-valence double- ζ quality reported PA(uracil) = 860–870 kJ mol⁻¹ [13–15].

What is the best value for the thermodynamic proton affinity of uracil? The experimental PA of uracil is given as 872.7 kJ mol⁻¹ in recent compilations [50, 51], which might indicate high accuracy. It is instructive to follow the evolution of this figure in the literature. The experimental grounds for the proton affinity of uracil were provided by bracketing measurements of Wilson and McCloskey who found that uracil was protonated by NH₄⁺ but not CH₃NH₃⁺ in a conventional CI source of a sector mass spectrometer [52]. Wilson and McCloskey estimated the PA of uracil between 207 and 216.3 kcal mol⁻¹ (866 and 905 kJ mol⁻¹, respectively) [52] on the then valid PA scale, which corresponds to 853–899 kJ mol⁻¹ on the current proton affinity scale [50, 51]. Lias and Levine narrowed these limits to the middle of the range and estimated PA (**1a**) as 870 kJ mol⁻¹ [53], a

value that was also used in the more recent complications of ion energy data, e.g., in 1988 [54], and furnished with additional significant figures in 1998 [49] and 1999 [51]. To the best of our knowledge, no recent experimental measurements have been reported that would support or justify the value and accuracy of the 872.7 kJ mol⁻¹ datum. As the closest analogy, the proton affinity of thymine was measured as 874 kJ mol⁻¹ by using the kinetic method [55]. If the effect on proton affinity of the methyl group in the uracil-thymine system is similar to that in the pyridine-picoline systems ($\Delta PA = 13\text{--}19$ kJ mol⁻¹) [51], the PA of uracil can be estimated at 855–861 kJ mol⁻¹. Considering the above experimental uncertainties, the proton affinities calculated by B3LYP, B3-MP2, and effective QCISD(T) methods are in agreement with experiment. In addition, PA = 858 kJ mol⁻¹ is the current benchmark for the most accurate estimate judged by the known performance of the computational methods and the levels of theory used [56].

Conclusions

Computational methods ranging from density-functional theory through Moller–Plesset theory up to quadratic configuration interaction identified structure **1a** as the most stable uracil tautomer, so it should predominate in the gas phase. The calculated topical proton affinities of uracil tautomers pointed to N-1-protonated 2,4-dihydroxypyrimidine as the most stable ion structure. The thermodynamic proton affinity of uracil, which is amenable to experimental measurements, was calculated as 858 kJ mol⁻¹ at the highest level of theory used in this work. This agrees with the results of the original bracketing measurements. We suggest that the PA value that was tabulated in recent compilations of thermochemical data should be remeasured to provide a reliable experimental datum to be compared with the calculated value.

Acknowledgments

Support of this work by the National Science Foundation (Grant CHE-9712570) is gratefully acknowledged. Computational support was provided by the Department of Chemistry Computer Cluster that received major funding from NSF (Grant CHE-9808182) and University of Washington.

References

- Fenn, J. B.; Mann, M.; Meng, C. K.; Wong, S. K.; Whitehouse, C. *Mass Spectrom. Rev.* **1990**, *9*, 37.
- Karas, M.; Hillenkamp, F. *Anal. Chem.* **1988**, *60*, 2299.
- Aue, D. H.; Bowers, M. T. In *Gas Phase Ion Chemistry*; Bowers, M. T., Ed.; Academic: New York, 1979; pp 1–51.
- Kebarle, P. *Annu. Rev. Phys. Chem.* **1977**, *28*, 445.
- Szulejko, J. A.; McMahan, T. B. *J. Am. Chem. Soc.* **1993**, *115*, 7839.
- Cooks, R. G.; Patrick, J. S.; Kotiaho, T.; McLuckey, S. A. *Mass Spectrom. Rev.* **1994**, *13*, 287.
- Turecek, F. *J. Mass Spectrom.* **1998**, *33*, 779.
- Nguyen, V. Q.; Turecek, F. *J. Mass Spectrom.* **1996**, *31*, 1173.

9. Nguyen, V. Q.; Turecek, F. *J. Mass Spectrom.* **1997**, *32*, 55.
10. Nguyen, V. Q.; Turecek, F. *J. Am. Chem. Soc.* **1997**, *119*, 2280.
11. Turecek, F. *J. Phys. Chem. A*, **1998**, *102*, 4703.
12. Nguyen, M. T.; Chandra, A. K.; Zeegers-Huyskens, T. *J. Chem. Soc., Faraday Trans.* **1998**, *94*, 1277.
13. Chandra, A. K.; Nguyen, M. T.; Zeegers-Huyskens, T. *J. Phys. Chem. A*, **1998**, *102*, 6010.
14. Chandra, A. K.; Nguyen, M. T.; Uchimaru, T.; Zeegers-Huyskens, T. *J. Phys. Chem. A*, **1999**, *103*, 8853.
15. Podolyan, Y.; Gorb, L.; Leszczynski, J. *J. Phys. Chem. A* **2000**, *104*, 7346.
16. Frisch, M. J.; Trucks, G. W.; Schlegel, H. B.; Gill, P. M. W.; Johnson, B. G.; Robb, M. A.; Cheeseman, J. R.; Keith, T. A.; Petersson, G. A.; Montgomery, J. A.; Raghavachari, K.; Al-Laham, M. A.; Zakrzewski, V. G.; Ortiz, J. V.; Foresman, J. B.; Cioslowski, J.; Stefanov, B. B.; Nanayakkara, A.; Challacombe, M.; Peng, C. Y.; Ayala, P. Y.; Chen, W.; Wong, M. W.; Andres, J. L.; Replogle, E. S.; Gomperts, R.; Martin, R. L.; Fox, D. J.; Binkley, J. S.; Defrees, D. J.; Baker, J.; Stewart, J. P.; Head-Gordon, M.; Gonzalez, C.; Pople, J. A. *Gaussian 94 (Revision D.1)*, Gaussian, Inc., Pittsburgh, PA, 1995.
17. Frisch, M. J.; Trucks, G. W.; Schlegel, H. B.; Scuseria, G. E.; Robb, M. A.; Cheeseman, J. R.; Zakrzewski, V. G.; Montgomery, J. A., Jr.; Stratmann, R. E.; Burant, J. C.; Dapprich, S.; Millam, J. M.; Daniels, A. D.; Kudin, K. N.; Strain, M. C.; Farkas, O.; Tomasi, J.; Barone, V.; Cossi, M.; Cammi, R.; Mennucci, B.; Pomelli, C.; Adamo, C.; Clifford, S.; Ochterski, J.; Petersson, G. A.; Ayala, P. Y.; Cui, Q.; Morokuma, K.; Malick, D. K.; Rabuck, A. D.; Raghavachari, K.; Foresman, J. B.; Cioslowski, J.; Ortiz, J. V.; Stefanov, B. B.; Liu, G.; Liashenko, A.; Piskorz, P.; Komaromi, I.; Gomperts, R.; Martin, R. L.; Fox, D. J.; Keith, T.; Al-Laham, M. A.; Peng, C. Y.; Nanayakkara, A.; Gonzalez, C.; Challacombe, M.; Gill, P. M. W.; Johnson, B.; Chen, W.; Wong, M. W.; Andres, J. L.; Gonzalez, C.; Head-Gordon, M.; Replogle, E. S.; Pople, J. A. *Gaussian 98, Revision A.6*, Gaussian, Inc., Pittsburgh PA, 1998.
18. Hehre, W. J.; Radom, L.; Schleyer, P. von R.; Pople, J. A. *Ab Initio Molecular Orbital Theory*; Wiley-Interscience: New York, 1986.
19. Parr, R. G.; Yang, W. *Density-Functional Theory of Atoms and Molecules*; Oxford University Press: New York, 1989.
20. Baerends, E. J.; Gritsenko, O. V. *J. Phys. Chem. A* **1997**, *101*, 5383.
21. Becke, A. D. *J. Chem. Phys.*, **1993**, *98*, 1372, 5648.
22. Stephens, P. J.; Devlin, F. J.; Chablowski, C. F.; Frisch, M. J. *J. Phys. Chem.* **1994**, *98*, 11623.
23. For the various frequency correction factors see for example: (a) Rauhut, G.; Pulay, P. *J. Phys. Chem.* **1995**, *99*, 3093. (b) Finley, J. W.; Stephens, P. J. *J. Mol. Struct. (THEOCHEM)* **1995**, *227*, 357. (c) Wong, M. W. *Chem. Phys. Lett.* **1996**, *256*, 391. (d) Scott, A. P.; Radom, L. *J. Phys. Chem.* **1996**, *100*, 16502.
24. Möller, C.; Plesset, M. S. *Phys. Rev.* **1934**, *46*, 618.
25. Pople, J. A.; Head-Gordon, M.; Raghavachari, K. *J. Chem. Phys.* **1987**, *87*, 5968.
26. Curtiss, L. A.; Raghavachari, K.; Pople, J. A. *J. Chem. Phys.* **1993**, *98*, 1293.
27. Smith, B. J.; Radom, L. *J. Phys. Chem.* **1995**, *99*, 6468.
28. Turecek, F.; Wolken, J. K. *J. Phys. Chem. A* **1999**, *103*, 1905.
29. Wolken, J. K.; Turecek, F. *J. Phys. Chem. A*, **1999**, *103*, 6268.
30. Wolken, J. K.; Turecek, F. *J. Am. Chem. Soc.* **1999**, *121*, 6010.
31. Turecek, F.; Carpenter, F. H. *J. Chem. Soc., Perkin Trans. 2* **1999**, 2315.
32. Turecek, F.; Polasek, M.; Frank, A. J.; Sadilek, M.; *J. Am. Chem. Soc.* **2000**, *122*, 2361.
33. Rablen, P. R. *J. Am. Chem. Soc.* **2000**, *122*, 357.
34. Tian, S. X.; Zhang, C. F.; Zhang, Z. J.; Chen, X. J.; Xu, K. Z. *Chem. Phys.* **1999**, *242*, 217.
35. Monshi, M.; Al-Farhan, K.; Al-Resayes, S.; Ghaith, A.; Hasanein, A. A. *Spectrochim. Acta A* **1997**, *53*, 2669.
36. Estrin, D. A.; Paglieri, L.; Corongiu, G. *J. Phys. Chem.* **1994**, *98*, 5653.
37. Leszczynski, J. *J. Phys. Chem.* **1992**, *96*, 1642.
38. Les, A.; Adamowicz, I. *J. Phys. Chem.* **1992**, *93*, 1649.
39. Leszczynski, J. *Int. J. Quantum Chem. Quantum Biol. Symp.* **1991**, *18*, 9.
40. Katritzky, A. R.; Karelson, M. *J. Am. Chem. Soc.* **1991**, *113*, 1561.
41. Jasien, P. G.; Fitzgerald, G. *J. Chem. Phys.* **1990**, *93*, 2554.
42. Gould, I. R.; Hiller, I. H. *J. Chem. Soc., Perkin Trans 2*, **1990**, 329.
43. Kwiatkowski, J. S.; Barlett, R. J.; Person, W. B. *J. Am. Chem. Soc.* **1988**, *110*, 2353.
44. Norinder, U. *J. Mol. Struct.* **1987**, *151*, 259.
45. Saunders, M.; Webb, G. A.; Tute, M. S. *J. Mol. Struct.* **1987**, *151*, 259.
46. Scanlan, M. J.; Hillier, I. H. *J. Am. Chem. Soc.* **1984**, *106*, 3737.
47. Zielinski, T. *Int. J. Quantum Chem.* **1982**, *22*, 639.
48. Czerminski, R.; Lesying, B.; Puhorille, A. *Int. J. Quantum Chem.* **1979**, *16*, 605.
49. (a) Dommrose, A.-F.; Grutzmacher, H.-F.; *Int. J. Mass Spectrom. Ion Processes* **1987**, *76*, 95. (b) Dommrose, A.-F.; Grutzmacher, H.-F. *Org. Mass Spectrom.* **1987**, *22*, 437. (c) Wolf, R.; Dommrose, A.-F.; Grutzmacher, H.-F. *Org. Mass Spectrom.* **1988**, *23*, 26. (d) Wolf, R.; Grutzmacher, H.-F. *Org. Mass Spectrom.* **1989**, *24*, 398. (e) Surig, T.; Grutzmacher, H.-F. *Org. Mass Spectrom.* **1990**, *25*, 446.
50. Hunter, E. P. L.; Lias, S. G. *J. Phys. Chem. Ref. Data* **1998**, *27*, 413.
51. *NIST Standard Reference Database Number 69–February 2000 Release*, Lindstrom, P. J.; Mallard, W. G., Eds.; <http://webbook.nist.gov/chemistry>.
52. Wilson, M. S.; McCloskey, J. A. *J. Am. Chem. Soc.* **1975**, *97*, 3436–3444.
53. Lias, S. G.; Liebman, J. F.; Levin, R. D. *J. Phys. Chem. Ref. Data* **1984**, *13*, 695.
54. Lias, S. G.; Bartmess, J. E.; Liebman, J. F.; Holmes, J. L.; Levin, R. D.; Mallard, G. W. *J. Phys. Chem. Ref. Data, Suppl No.1* **1988**, *17*, 145.
55. Greco, F.; Liguori, A.; Sindona, G.; Ucella, N. *J. Am. Chem. Soc.* **1990**, *112*, 9092.
56. Smith, B. J.; Radom, L. *Chem. Phys. Lett.* **1994**, *231*, 345.